JOURNAL OF PROPULSION AND POWER
Vol. 14, No. 2, March–April 1998

Propellant Utilization in Hall Thrusters

Y. Raitses* and J. Ashkenazy*
Soreq Nuclear Research Center, Yavne 81800, Israel
and
M. Guelman†
Technion—Israel Institute of Technology, Technion City, Haifa 32000, Israel

Fuel-optimal trajectories for electrically propelled spacecraft require a varying thrust trajectory. To achieve this requirement, the electric thruster has to be operated with a variable thrust-to-power ratio at the maximum available input power. To implement this operating mode with a Hall thruster it is necessary to modify both the mass flow rate and the discharge voltage during the flight time. A crucial problem associated with Hall thruster operation in a variable-thrust mode is the degradation of thruster performance under mass flow rate variations. Experiments with a laboratory Hall thruster have indicated that this degradation is mainly caused by a reduction of the propellant utilization at lower values of the mass flow rate. By modifying the channel geometry, namely, the channel length and channel profile, improvements in the behavior of the propellant utilization at small mass flow rates and, consequently, an improved thruster performance have been achieved. Results of experimental tests of a Hall thruster at various operating points and geometry are presented.

Introduction

THERE has been an increasing appreciation of the use of Hall thrusters for spacecraft orbit control as a way to reduce the initial spacecraft mass and/or to extend the operating lifetime of satellites. Most of the research effort has been devoted to verify the performance of existing Hall thrusters (SPT) and their qualification for potential space applications.[1,2] Results inspired conceptual and detailed orbit transfer studies with Hall-thruster-propelled spacecraft.[3,4] In most of these studies, spacecraft orbit control is based on Hall-type thrusters operating with a constant thrust-to-input power ratio during the flight time.

As an alternative to Hall thruster operation at a constant thrust-to-power ratio, a different approach was proposed for orbit transfer of an electrically propelled spacecraft employing Hall thrusters.[5–7] Applying optimal thrust acceleration control enables the minimization of the propellant expenditure and, as a result, the reduction of the initial spacecraft mass. To realize this control it is necessary to vary the thrust level, at the maximum available power, during the flight time. The results described in Refs. 6 and 7 demonstrate that power-limited optimal control of Hall thruster propulsion enables the implementation of very small spacecraft for various space missions.

The possibility of Hall thruster operation in a variable thrust mode has been studied in Ref. 8. Efficient Hall thruster operation is necessary to minimize the propellant requirements for the mission. A simplified analytical solution for the propellant utilization in Hall thrusters is described in Ref. 9. A study of the effect of thruster input parameters (mass flow rate, input power, and magnetic field strength) on thruster performance was described in Ref. 10. A laboratory model Hall thruster was used to characterize the thruster performance with xenon propellant in a broad operating range. Generally speaking, the thrust, specific impulse, and efficiency were found to decrease as the mass flow rate was reduced. This behavior was attributed to the reduction in ionization probability at low mass flow rates, resulting in a reduced propellant utilization.

The preceding results indicated that a Hall thruster with a simple, fixed configuration can demonstrate high performance across a limited range of mass flow rate values. Therefore, it seems that variable thrust operation at a constant input power is not practical with these thrusters unless modifications in the thruster configuration can be implemented to help overcome present limitations. As the first step toward this goal we focused on the investigation of the effect of the channel length[11] and profile on thruster operation under various operating conditions, with an emphasis on understanding the physical processes affecting the propellant utilization. Results of this investigation are described in the present paper.

Effect of Channel Geometry on Propellant Utilization

A schematic drawing of the Hall thruster is shown in Fig. 1. The thruster has a coaxial geometry and consists of four main parts: 1) anode, 2) cathode-neutralizer, 3) magnetic circuit, and 4) a channel made of insulator material. The propellant injected into the channel is ionized and accelerated by the combined effects of electric and magnetic fields. The propellant utilization, i.e., the fraction of propellant mass that is ionized and accelerated, is determined by the ionization probability and ion losses in the channel and, therefore, depends on its geometry.[8,9] Changes in channel geometry can be implemented by modifying the channel length or its profile.

The variation of the channel length could affect the propellant utilization at different mass flow rate values. When the mass flow rate is reduced, and as a result the ionization mean free path of the propellant atoms is extended, the ionization probability can be expected to be larger in a longer channel. On the other hand, length-dependent ion losses could also be increased in a longer channel. Therefore, it could be expected that for different values of the mass flow rate, there is an optimum channel length for which the propellant utilization is maximal. In practice, the channel length, taken from the anode front to the thruster exhaust, can be varied by changing the position of the anode in the channel (Fig. 2a).

Received July 26, 1996; revision received Aug. 4, 1997; accepted for publication Oct. 14, 1997.

*Research Scientist, Propulsion Physics Laboratory. Member AIAA.

†Professor, Asher Space Research Institute, Faculty of Aerospace Engineering. Member AIAA.

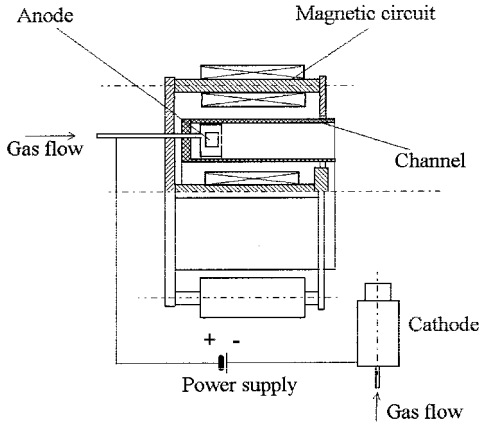

Fig. 1 Schematic drawing of the Hall thruster.

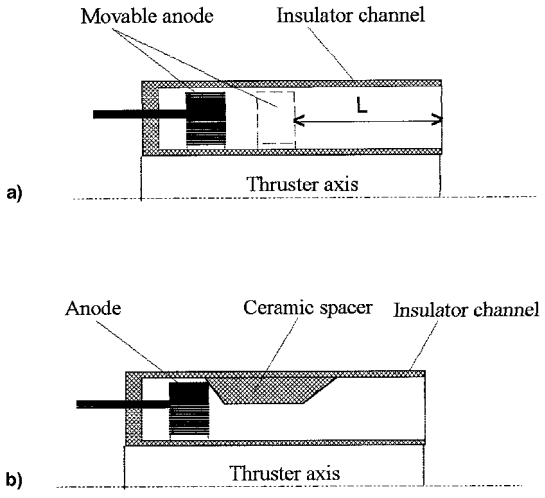

Fig. 2 Two kinds of channel geometry variations: a) length, by changing the anode position, and b) profile, by inserting a spacer into the near anode region.

As for the channel profile, the ionization probability could be affected by the height of the channel in the near-anode region. If the near-anode channel cross section is narrowed, the flux density of electrons, diffusing toward the anode, is expected to increase. This would result in an increase in the ionization probability because of the increased rate of ionizing collisions. Near the exhaust (acceleration region), however, it seems preferable for the height of the channel to be wider to reduce wall losses. Electron flux losses, causing reduced propellant utilization, could also result from a sharp boundary between the regions with different heights. It was suggested that these losses could be reduced by a proper channel profile that would smooth the transition between the regions. In the present experiments, the channel profile was modified by inserting a cylindrical ceramic spacer inside the channel (Fig. 2b).

Experimental Setup

Test Facility

The thruster operation experiments were performed in a 1.2 $\times$ 2 m stainless-steel vacuum chamber equipped with a two-stage roots-pump system and a diffusion pump with a nominal pumping speed of 17,500 l/s of air (without trap). The vacuum in the chamber was monitored with an ion gauge. With no mass flow, a vacuum better than 10^{-4} Pa was obtained in the chamber. During xenon mass flow of 1.2 mg/s, a vacuum of 3.5×10^{-3} Pa was obtained, corresponding to a xenon pumping speed of about 5700 l/s.

The propellant system serves to supply and control the propellant flow from a gas tank to the anode and cathode. For that purpose, a commercial mass flow control and measurement system, calibrated for xenon, is used. This system includes two Tylan FC-260 controllers (0-80 SCCM for the anode and 0-20 SCCM for the cathode) with valves and the Tylan RO28 readout and control box. According to the manufacturer, the accuracy of the FC-260 controller is 1%. Separate laboratory power supplies are used to provide the discharge ignition, support main discharge, and bias the magnetic coils. The discharge voltage and current and the coils current are measured with standard shunts, using commercial high-accuracy (less than 0.4%) multimeters.

Thruster

A laboratory model Hall thruster is used as a research tool to characterize the thruster operation in a variable thrust mode under different channel geometry variations. The magnetic circuit of the laboratory thruster consists of a modular magnetic core fabricated from a low carbon steel, and external and internal electromagnetic coils (Fig. 1). The coils are connected in series to the bias power supply. The magnetic field distribution along the channel median is shown in Ref. 10. Generally speaking, it increases toward the channel exhaust with the maximum obtained between the external and internal poles. At a coil current of 1 A, a magnetic field strength of 0.007 T is obtained in the middle of the gap between the poles.

The coaxial channel is made of a machinable glass ceramics. Its external diameter is about 70 mm, which is appropriate for the subkilowatt power range[12] whereas the full length taken from its back wall to the exhaust is about 50 mm. The annular anode has a second role as the distributor of the propellant in the thruster channel. The construction of the anode enables it to move in the channel. A hollow-type LaB_6 cathode is used to initiate and support the discharge in the thruster and to neutralize the ion flux from the channel.

As shown in Fig. 2a, the channel length can be modified by changing the position of the anode in the channel. Two glass ceramics spacers of different thickness that narrow the channel by 40 and 55%, respectively, in the near-anode region, were used to modify the channel profile (Fig. 2b). Each spacer extends from the anode to a point where the magnetic field strength is roughly half its magnitude between the poles. In addition, both spacers have a wedge-like shape at their outer side.

Diagnostic Setup

Thrust measurements are performed with a pendulum-type thrust stand[10] on the arm of which the thruster is suspended. A high-sensitivity inclinometer, located at the fulcrum, is used to accurately measure the arm deflection angle, and thus to indicate the thrust. Thrust stand calibrations were performed throughout these experiments each time the thruster geometry was changed. For this purpose, a weight arrangement was used that enabled the calibration of the thrust stand in the equivalent thrust range of up to 60 mN. In these calibrations, the thrust stand exhibited a very good linearity, and a better than 1% reproducibility. The smallest difference between calibrating weights that was reliably detected from the corresponding deviations of the inclinometer output, was equivalent to a thrust of 0.2 mN. However, because the smallest directly measured calibrating weight was equivalent to a thrust of 0.5 mN, this value was taken as the thrust resolution. The thermally induced zero drift of the thrust stand during thruster operation was typically 1 mN or less after 1 h of operation.

In addition to the measurements of the thrust, mass flow rate, discharge voltage and current, the angular ion flux distribution was measured using a planar langmuir probe. The probe is a circular disk made of a low-sputtering tungsten–copper alloy with a collecting area of 3.14 cm^2. The probe is mounted on

a rotating arm that enables it to move the probe on a circle whose center is on the thruster axis, and its radius, measured to the collecting surface of the probe, is 32 cm. During the thruster operation, the probe motion is implemented with an electric motor, and its angular position is monitored with a linear high-resolution potentiometer. The probe is negatively biased with a voltage-regulated power supply. The probe current was deduced from the voltage drop on a 100 Ω shunt resistor. To estimate the total ion current, and thus to deduce the propellant utilization, we assumed that the ion flux from the thruster was axially symmetric. Then, by interpolating and integrating over the measured flux distribution, the total ion current at the thruster exhaust I_i can be obtained. A personal computer-based data acquisition system is used to control the probe position, to measure the probe current, and to obtain the total ion current.

Thruster Operation Experiments

The measurements include thruster operation with three channel lengths, L = 20, 30, and 40 mm, and thruster operation with two spacers of different thickness (L = 30 mm). These measurements were performed in the xenon mass flow rate range of 0.9–2.17 mg/s, a discharge voltage of 150–500 V, and a magnetic coils' current of 0.5–5 A. At this range of the mass flow rate, the background pressure measured in the vacuum chamber was between 3×10^{-3} and 8.3×10^{-3} Pa. No attempt was made in these experiments to optimize the mass flow rate through the cathode, as the purpose of this work was to investigate the ionization and acceleration processes. Therefore, the value of the mass flow rate $\dot{m}$ in all of the results described later in this paper include only the anode mass flow rate and a correction for the background pressure in the chamber,[13] which, under the conditions of our vacuum facility, is a little more than 2% of the anode mass flow rate,[10] while cathode mass flow rate is not included.

Procedure of Measurements

When the thruster is turned on visual inspection serves to verify the existence of a jet, its stability, and azimuthal homogeneity. After the thruster and thrust stand are both in a thermal steady state (several tens of minutes), the measurements are initiated. The discharge current and thrust were measured under various values of the coils' current at given mass flow rate and discharge voltage values, and the minimum discharge current value was found. Then, the discharge voltage was varied and this set of measurements was repeated.

At certain operating points, the angular ion flux distribution was also measured. For this purpose, the probe voltage–current (V–I) characteristics were measured at different probe positions and under various operating conditions of the thruster. In most of these measurements, a saturation of the ion current was clearly observed when the negative bias was below -10 V, with respect to the ground. Between -10 and -40 V, the relative change was less than 2%, indicating that the secondary electron emission from the probe is not significant in this voltage range. Based on this result, the angular flux distribution measurements were performed with a constant bias voltage of -30 V.

The propellant utilization $\eta_p = m_a I_i / e\dot{m}$, at each operating point, was deduced from the mass flow rate $\dot{m}$ and from the ion current I_i obtained from the angular ion flux distribution measurement as described earlier. m_a is the mass of a propellant atom, and e is the electron charge. The specific impulse, $Isp = T/\dot{m}g$, and thruster efficiency, $\eta_T = T^2/2\dot{m}P_e$, were deduced from the measured thrust T, input power P_e, and the mass flow rate. Through all of these measurements, which took about 200 h of thruster operation, the same channel was used, thus avoiding uncertainties related to differences in the channel material and machining. At the end of this set of measurements, the first measurements were repeated with no observable differences. Moreover, in the channel profile variation experiments, inspection at the end of the measurements with each inserted spacer indicated that there were no changes in its position relative to the thruster exhaust and no observable erosion of its surface.

Uncertainties in Thruster Integral Characteristics

The relative error in the thrust is equal to the ratio of the thrust resolution (0.5 mN) to the measured thrust magnitude, and thus it tends to decrease when the thrust magnitude increases. For example, in the thrust range of 10–50 mN, its value drops from 5 to 1%. The accuracy of power measurements is better than 0.5%. Following Ref. 13, we assume that the uncertainty in the determination of the background mass flow rate is 100%. Hence, for our propellant system, the error in determination of the total mass flow rate is less than 2.4%. Then, the relative specific impulse and efficiency errors at the previously specified thrust range are 5.5–2.6% and 10.3–3.2%, respectively.

There are a number of issues that cause uncertainties with regard to the accuracy of the ion flux distribution measurement process described earlier. These include the following:

1) The probe efficiency, i.e., what fraction of the ion current at the probe is being collected.

2) Because of the modest size of our present vacuum chamber, and to avoid backflow effects, the probe is located relatively close to the thruster ($\approx$30 cm). The question then is to what extent does the flow behave asymptotically at this distance and what effect does it have on the accuracy of the obtained value of the total ion current.

3) Ion exchange in the plume and its dependence on the background pressure in the chamber is an uncertainty.

4) Lastly, the double ion fraction is a concern.

Though these issues remain unresolved in the present work, it was nevertheless assumed that for the purpose of comparing thruster operation between different thruster configurations and/or operating conditions, the results of probe measurements could be used, provided they are performed by the same probe setup, at the same distance between the thruster and the probe and when changes in the vacuum background pressure, affected by varying the mass flow rate, are not significant. This assumption is similar to that suggested and demonstrated in Ref. 14, which describes probe measurements of a Hall thruster with a probe setup and vacuum facility similar to ours.

Results and Discussions

In the experiments described next, it was observed systematically that when the coils' current is varied at a fixed discharge voltage and mass flow rate, there is a value of this current for which the discharge current is minimal, a behavior, that is typical for Hall thrusters.[10,12] Because, under these coils current variations, changes in the thrust magnitude are typically less than those in the discharge current, the thruster efficiency at this value of the coils' current is maximal. Therefore, all of the results presented next represent thruster performance at the measured minimum discharge current vs the coils' current point for the given mass flow rate and discharge voltage values.

Channel Length Variations

Figures 3–5 show the propellant utilization, specific impulse, and thruster efficiency vs the anode mass flow rate for the three channel length cases, L = 20, 30, and 40 mm. Figures 3–5 illustrate the results obtained at three values of the discharge voltage, V_d = 200, 250, and 300 V.

As seen from Fig. 3, for all three channel length cases, the propellant utilization is reduced as the mass flow rate is varied from 2.17 to 0.9 mg/s at a constant discharge voltage. For example, at L = 20 mm, the propellant utilization measured for V_d = 300 V is reduced from 0.8 to 0.6. This behavior is obviously a result of the reduction in the ionization probability

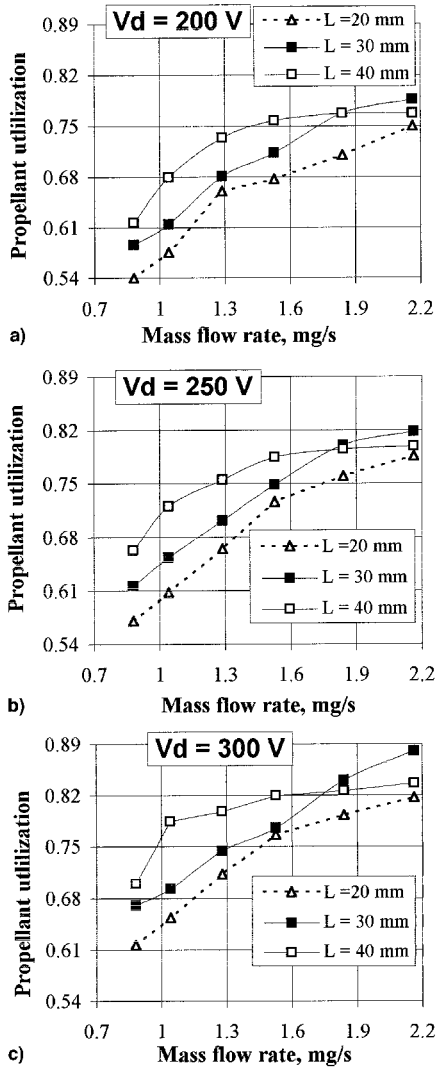

Fig. 3 Propellant utilization vs the mass flow rate obtained with the three channel lengths, L = 20, 30, and 40 mm, at three discharge voltages.

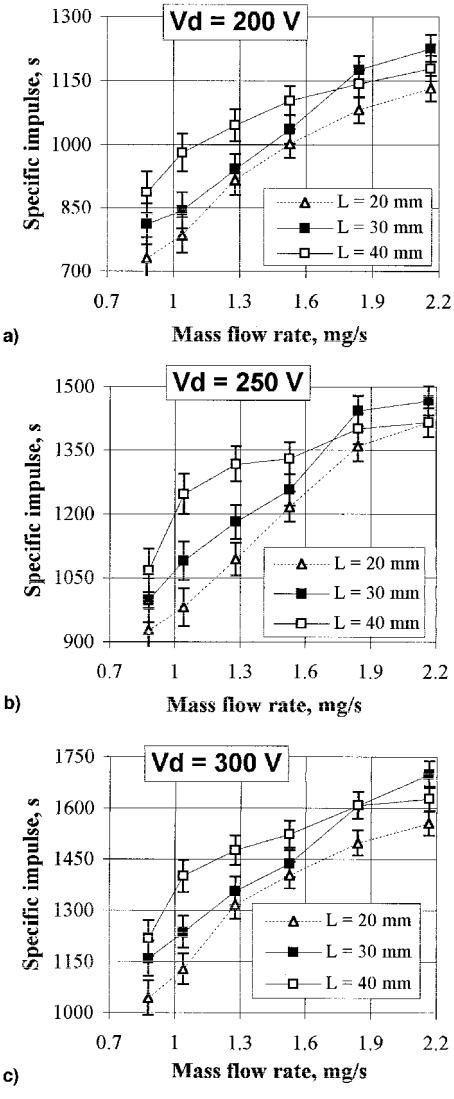

Fig. 4 Specific impulse vs the mass flow rate obtained with the three channel lengths, L = 20, 30, and 40 mm, at three discharge voltages.

as the mass flow rate is reduced. It can be seen also that at mass flow rates of less than 1.84 mg/s, the propellant utilization increases with the channel length, the largest difference being at about 1.1 mg/s. Below this value, it seems that even a channel length of 40 mm is not long enough to provide high ionization probability. Above 1.84 mg/s, the largest propellant utilization was obtained with L = 30 mm. At these large mass flow rate values, the ionization probability is probably high in both the L = 30 and 40 mm cases, but not in the L = 20 mm case. The lower propellant utilization in the L = 40 mm case could be a result of increased length-dependent losses, such as ion and electron losses.

The specific impulse and thruster efficiency vs the mass flow rate are shown in Figs. 4 and 5, respectively. For a fixed channel length and a constant discharge voltage, both the specific impulse and thruster efficiency increase with the mass flow rate. Similar to the propellant utilization, the better results were obtained at small mass flow rates with L = 40 mm, whereas the higher thruster performance was obtained at larger mass flow rates with L = 30 mm.

At a constant discharge voltage, the specific impulse is essentially proportional to the propellant utilization. Therefore, it is interesting to compare the behavior of the specific impulse and the propellant utilization under mass flow rate and channel length variations. Generally speaking, for a fixed channel length and at a given value of the discharge voltage, the specific impulse behaves similar to the propellant utilization. For example, at a discharge voltage of 250 V, as the mass flow rate is varied from 2.17 to 1.05 mg/s, the propellant utilization (Fig. 3b) is reduced by a factor of 1.3 at L = 20 mm, 1.26 at L = 30 mm, and 1.1 at L = 40 mm. For the same discharge voltage and mass flow rate changes, the specific impulse is decreased by a factor of 1.5 at L = 20 mm, 1.4 at L = 30 mm, and 1.18 at L = 40 mm (Fig. 4b). These results demonstrate that at a simple, fixed thruster configuration, the degradation of thruster performance is mainly a result of the reduced ionization probability at lower mass flow rates.

The influence of the discharge voltage on the propellant utilization can be analyzed by comparing the results shown in Fig. 3. As can be seen, for a given channel length and a fixed mass flow rate, there is almost an insignificant increase in the propellant utilization when the discharge voltage is varied from 200 to 300 V. This behavior is in agreement with the measured V–I characteristics under different mass flow rates.[11] As for the specific impulse, for given channel length and mass flow rate, it increases with the discharge voltage. For example, for L = 40 mm and $\dot{m}$ = 1.84 mg/s, the specific impulse increases from 1140 to 1600 s as the voltage is increased from 200 to 300 V. This increase is somewhat beyond what would be expected from a $\sqrt{V_d}$ dependence, even when the small difference in the propellant utilization is taken into account. This may be a result of a larger fraction of the applied discharge

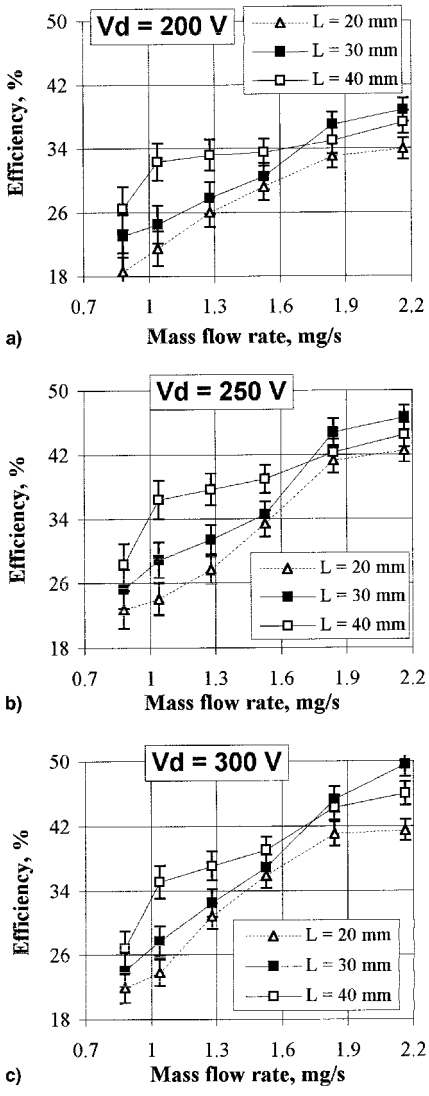

Fig. 5 Thruster efficiency vs the mass flow rate obtained with the three channel lengths, L = 20, 30, and 40 mm, at three discharge voltages.

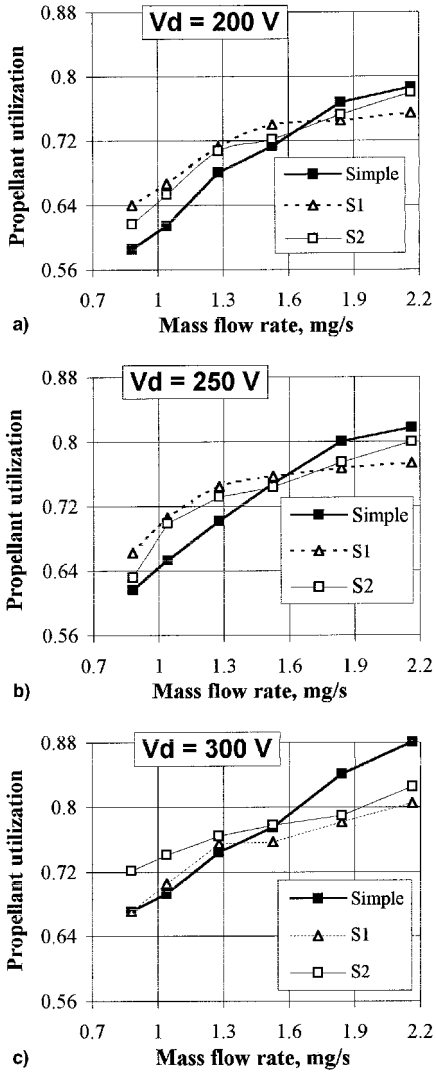

Fig. 6 Propellant utilization vs the mass flow rate obtained with two different spacers. S1 (a 40% reduction in the channel cross section in the near-anode region) and S2 (a 55% reduction), and with a simple channel profile of the same length (L = 30 mm).

voltage being exploited in the acceleration process.[12] As for the thruster efficiency (Fig. 5), at mass flow rates larger than 1.5 mg/s, the efficiency increases with the discharge voltage, while at smaller mass flow rates, higher efficiency was obtained at V_d = 250 V. The reduced thruster efficiency obtained for small mass flow rates at the larger discharge voltage may be a result of near-wall or instability processes,[12] which could cause an increase in the discharge current.

Channel Profile Variations

Results of experiments with two different spacers, S1 (a 40% reduction in the channel cross section in the near-anode region) and S2 (a 55% reduction), and a comparison with the case of a simple channel of the same channel length (L = 30 mm) is described next. Figures 6–8 compare the propellant utilization, specific impulse, and thruster efficiency vs the mass flow rate, obtained with the two spacers and the simple channel, for three values of the discharge voltage: V_d = 200, 250, 300 V.

Figure 6 shows that, as in the case of the simple channel, as the mass flow rate is reduced, the propellant utilization decreases in the two spacer cases, leading to a similar behavior of the specific impulse and efficiency (Figs. 7 and 8). Nevertheless, the insertion of the spacers led to improvements in the propellant utilization and thruster performance at low mass flow rates, which were more significant at 200 and 250 V. At large mass flow rates, the better propellant utilization and thruster performance were obtained with the simple channel. It is our opinion that this behavior, which is analogous to the dependence on the channel length, justifies the assumption that at small mass flow rates the narrowing of the near-anode region improves the ionization probability. At larger mass flow rates the ionization probability is high enough in the simple channel and, again, losses to the channel seem to be the important factor. These include ion losses, as demonstrated in Fig. 6, and also, most probably, electron losses, as indicated by the increase in the total discharge current that we observed with the spacers at the relevant operating points. As can be seen at 300 V, the improvements in the propellant utilization at low mass flow rates, as a result of the insertion of the spacers (Fig. 6c), are not reflected in the thruster efficiency (Fig. 8c). This is associated with an increase in the discharge current beyond the increase in the ion current observed at the relevant operating points. The reasons for this behavior are not clear.

As evident from Figs. 7 and 8, the differences between the specific impulse and the efficiency obtained with and without a spacer are in some cases smaller than the error bars. Nevertheless, the preceding conclusions are valid for the following reasons. First, as already described, although the error bars are calculated based on a thrust resolution of 0.5 mN, a smaller thrust difference ($\geq$0.2 mN) could be reliably detected in com-

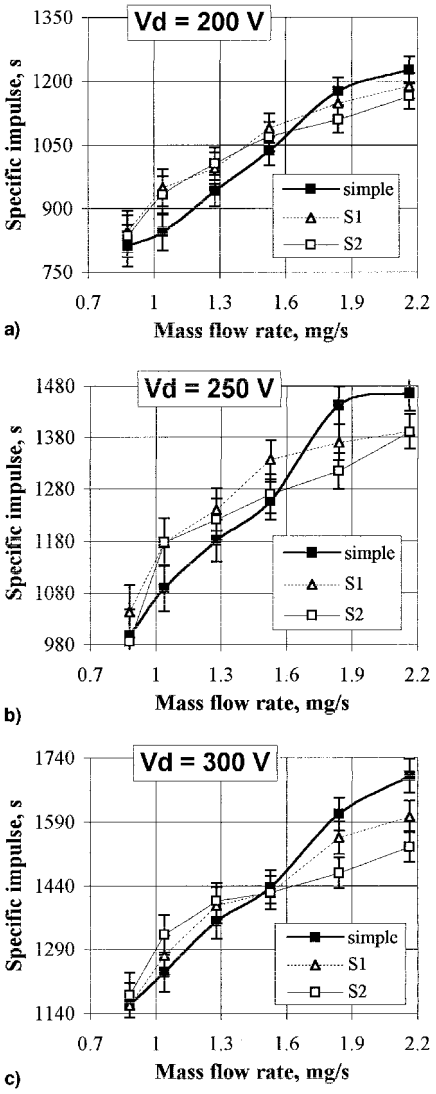

Fig. 7 Specific impulse vs the mass flow rate obtained with two different spacers: S1 (a 40% reduction in the channel cross-section in the near-anode region) and S2 (a 55% reduction), and with a simple channel profile of the same length (L = 30 mm).

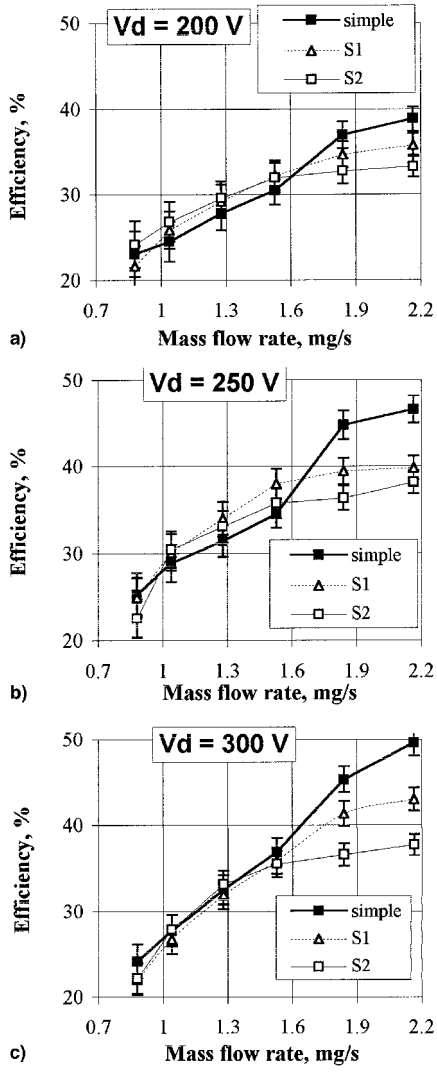

Fig. 8 Thruster efficiency vs the mass flow rate obtained with two different spacers: S1 (a 40% reduction in the channel cross section in the near-anode region) and S2 (a 55% reduction), and with a simple channel profile of the same length (L = 30 mm).

parative measurements. Second, the same type of behavior, in particular the improvements in the specific impulse and efficiency at low mass flow rates with the addition of spacers, was repeated in all three values of the discharge voltage (except for the efficiency at 300 V).

Thruster Operation at a Constant Input Power

The preceding results indicate that channel length and profile variations can improve the thruster performance at small mass flow rates. As expected, both types of channel geometry variations affect the thruster performance mainly because of changes in the propellant utilization. At mass flow rates of less than 1.84 mg/s, the best results were obtained with the longer channel, L = 40 mm. Nevertheless, in experiments with the thinner spacer the results obtained at V_d = 250 V and in the mass flow rate range of 1.3–1.5 mg/s are close to those obtained with L = 40 mm. Furthermore, in at least one case, V_d = 270 V and $\dot{m}$ = 1.5 mg/s, the specific impulse obtained with the spacer was larger than with the longer channel, 1400 vs 1330 s. Ultimately, at larger mass flow rates, the best results were obtained with the simple L = 30-mm case.

When considering the possibility of Hall thruster operation in a variable thrust mode, it is interesting to compare the thruster performance obtained at a constant input power between a simple, fixed channel geometry and the best results obtained in experiments with channel geometry variations. For example, Fig. 9 compares the thrust, specific impulse, and thruster efficiency vs the mass flow rate at an input power of 430 ± 15 W, between the thruster with a fixed channel geometry (L = 30 mm) and a hypothetical thruster with a movable anode and, thus, with a variable channel length (L = 30 and 40 mm). The points on these curves represent various discharge voltage values. That is because as the mass flow rate changes so does the discharge current and, thus, the discharge voltage has to be changed in accordance to keep the input power constant. As can be seen from Fig. 9 there is an overall improvement in thruster performance of the variable configuration compared to the fixed one. Nevertheless, as Fig. 9c shows, this improvement is not enough to keep the thruster efficiency constant at a large value. In accordance with this result the increase of the specific impulse, when the mass flow rate is reduced, is less than the expected $\sqrt{V_d}$ factor.

At this stage, it is not clear what the scaling relations are between the channel length and profile, the mass flow rate, and the discharge voltage, and how these relations can be optimized for an efficient Hall thruster operation, for example, in a variable thrust mode. For this purpose, theoretical modeling, which could enable scaling between the thruster input and output parameters and their dependence on the thruster configuration, is certainly needed.

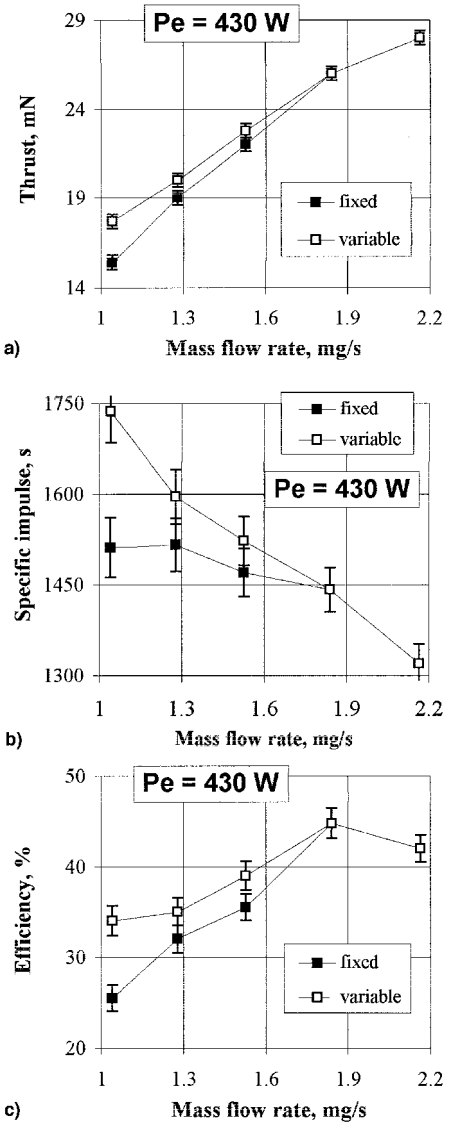

Fig. 9 Hall thruster operation at a constant input power of 430 ± 15 W and at a variable thrust mode with a fixed channel geometry (L = 30 mm) and a variable channel length (L = 30 and 40 mm): a) thrust, b) specific impulse, and c) efficiency vs the mass flow rate.

Conclusions

As an alternative to Hall thruster operation at a constant thrust-to-power ratio, the possibility of efficiently operating this type of thruster in a variable thrust mode was studied. To implement this mode it is necessary to vary, at the same time, the mass flow rate, discharge voltage, and magnetic field strength. In this paper results of thruster measurements made under various operating conditions and with channel geometry variations both in length and profile have been presented. The results obtained for three different channel lengths substantiate our proposition that the observed dependence of the propellant utilization and the thruster performance on the channel length is mainly a result of differences in the ionization probability and length-dependent losses. The conclusion to be derived from these results is that to achieve effective propellant utilization in Hall thrusters the channel length has to be optimized for specific operating conditions. Moreover, a comparison between thruster operation with the two spacers indicates that the channel profile could also be used as a means to improve the propellant utilization and thruster performance at small mass flow rates.

Acknowledgment

The authors thank G. Appelbaum for his excellent technical assistance.

References

[1]Pencil, E. J., Randolph, T., and Manzella, D. H., "End-of-Life Stationary Plasma Thruster Far-Field Plume Characterization," AIAA Paper 96-2709, July 1996.

[2]Sankovic, J. M., Haag, T. W., and Manzella, D. H., "Performance Evaluation of a 4.5 kW SPT Thruster," 24th International Electric Propulsion Conf., IEPC-95-30, Moscow, Russia, Sept. 1995.

[3]Warwick, R., "SEP Mission to Detect Water Ice in the Lunar Polar Regions," AIAA Paper 95-2816, July 1995.

[4]Fedotov, G. G., Konstantinov, M. S., and Petukhov, V. G., "Design of Solar-Powered Low Thrust Pluto Flyby Trajectories," 45th Congress of the International Astronautical Federation, IAF-94-A.6.052, Jerusalem, Israel, Oct. 1994.

[5]Guelman, M., "Earth-to-Moon Transfer with a Limited Power Engine," *Journal of Guidance, Control, and Dynamics*, Vol. 18, No. 5, 1995, pp. 492–496.

[6]Guelman, M., Ashkenazy, J., and Raitses, Y., "From Earth to Moon with Electric Propulsion," 45th Congress of the International Astronautical Federation, IAF-94-A.6.050, Jerusalem, Israel, Oct. 1994.

[7]Golan, O., Milegur, E., Arad, D. Kivelevitch, E., Kochavi, E., Kopelman, I., Riechman, A., Sadeh, Z., Shlachetzki, V., and Zango, A., "Low Thrust Mission to Phobos," *Proceedings of the 36th Israel Annual Conference on Aerospace Sciences* (Israel), Technion—Israel Inst. of Technology, Haifa, Israel, 1996, pp. 498–503.

[8]Raitses, Y., Ashkenazy, J., and Guelman, M., "Hall Thruster Operation in a Variable Thrust Mode," *Proceedings of the 36th Israel Annual Conference on Aerospace Sciences* (Israel), Technion—Israel Inst. of Technology, Haifa, Israel, 1996, pp. 446–454.

[9]Raitses, Y., and Ashkenazy, J., "Discharge Characteristics of Hall Current Accelerators," *Proceedings of the 17th International Symposium on Discharges and Electrical Insulation in Vacuum* (Berkeley, CA), Inst. of Electrical and Electronics Engineers, New York, 1996, pp. 492–496.

[10]Ashkenazy, J., Raitses, Y., and Appelbaum, G., "Investigations of a Laboratory Model Hall Thruster," AIAA Paper 95-2673, July 1995.

[11]Ashkenazy, J., Raitses, Y., Appelbaum, G., and Guelman, M., "Study and Diagnostics of the Effect of Length Variation in Hall Thrusters," 24th International Electric Propulsion Conf., IEPC-95-29, Moscow, Russia, Sept. 1995.

[12]Bugrova, A. I., Kim, V., Maslennikov, N. A., and Morozov, A. I., "Physical Processes and Characteristics of Stationary Plasma Thrusters with Closed Electron Drift," 22nd International Electric Propulsion Conf., IEPC-91-79, Viareggio, Italy, Oct. 1991.

[13]Brophy, J. R., "Stationary Plasma Thruster Evaluation in Russia," Jet Propulsion Lab., JPL-92-4, Pasadena, CA, March 1992.

[14]Borisov, B. S., Mikhaylov, K. K., Rusakov, A. V., Semenkin, A. V., and Chislov, H. O., "Experimental Study of Exhaust Beam of Anode Layer Thruster," 24th International Electric Propulsion Conf., IEPC-95-51, Moscow, Russia, Sept. 1995.